Chem Soc Rev

Recent Progress of Abrasion-Resistant Materials: Learning from Nature

Journal:	*Chemical Society Reviews*
Manuscript ID:	CS-REV-06-2015-000459.R1
Article Type:	Tutorial Review
Date Submitted by the Author:	20-Aug-2015
Complete List of Authors:	Meng, Jingxin; Technical Institute of Physics and Chemistry, Chinese Academy of Science, Laboratory of Bio-inspired Smart Interface Science Zhang, Pengchao; Institute of Chemistry, Chinese Academy of Sciences, Wang, Shutao; Technical Institute of Physics and Chemistry, Chinese Academy of Science, Laboratory of Bio-inspired Smart Interface Science,

Chem Soc Rev

TUTORIAL REVIEW

Recent Progress of Abrasion-Resistant Materials: Learning from Nature

Received 00th January 20xx,
Accepted 00th January 20xx

DOI: 10.1039/x0xx00000x

www.rsc.org/

Jingxin Meng,[a] Pengchao Zhang [b] and Shutao Wang*[a]

Abrasion-Resistant materials have attracted great attention for their widely applications in industry, biomedicine and military. However, it remains a great challenge to develop abrasion-resistant materials along with unique features such as lightweight and flexibility to satisfy the unmet demands. The outstanding performance of natural abrasion-resistant materials motivates the new development of bio-inspired abrasion-resistant materials. This review summarizes the recent progress in the investigation of natural abrasion-resistant materials to explore their general design principle (*i.e.*, the correlation between chemical components and structural feature). Following natural design principle, several artificial abrasion-resistant materials have shown unique abrasion-resistant properties. The potential challenge in future and possible solutions of designing bio-inspired abrasion-resistant materials are also briefly discussed.

Key learning points

1. The theoretical basis for assessing abrasion resistance.
2. Chemical design of abrasion-resistant materials in nature.
3. Structural design of abrasion-resistant materials in nature.
4. Following natural design principle, the fabrication and characterization of several bio-inspired abrasion-resistant materials.
5. Future challenges and opportunities on the development of new artificial abrasion-resistant materials.

1. Introduction

Abrasion-resistant materials are of significant interest in various fields, such as industrial devices, biomedical materials, and military

[a.] *Laboratory of Bio-inspired Smart Interface Science, Technical Institute of Physics and Chemistry, Chinese Academy of Science, Beijing, 100190, P. R. China*
E-mail: stwang@mail.ipc.ac.cn; Fax: +86-10-82627566; Tel: +86-10-82543658.
[b.] *Beijing National Laboratory for Molecular Sciences (BNLMS), Key Laboratory of Organic Solids Institute of Chemistry, Chinese Academy of Sciences, Beijing, 100190, P. R. China*

Abrasion-resistant materials are of significant interest in various fields, such as industrial devices, biomedical materials, and military equipments, because they have outstanding capability to tolerate great loading with negligible loss or damage of materials during a sliding, rolling, or impact events.[1] Traditional abrasion-resistant materials mainly introduce hard coating (*e.g.*, Al_2O_3, TiN/NbN and NbN/VN) to enhance the abrasion resistance.[2] However, these abrasion-resistant materials can't satisfy some special purposes,

Jingxin Meng

Jingxin Meng is currently an assistant professor at Technical Institute of Physics and Chemistry, Chinese Academy of Sciences (TIPCCAS). He received his Ph.D. degree (2011) in inorganic chemistry from Northeast Normal University under the supervision of Prof. Enbo Wang. Then, he worked as a postdoctoral researcher with Prof. Shutao Wang at the Institute of Chemistry, Chinese Academy of Sciences (ICCAS) (2011-2014). His current research focuses on designing bio-inspired interfacial materials with controllable abrasion and adhesion.

Pengchao Zhang

Pengchao Zhang is currently a PhD student at ICCAS. He received his BS in materials science from Wuhan University of Technology, China, in 2010. Then, he joined ICCAS under the supervision of Prof. Lei Jiang and Prof. Shutao Wang. He is interested in the construction and application of bio-inspired micro/nano-surfaces with special wettability/adhesion towards anisotropic sliding of water drops, fabricating of thin polymer films, and detecting rare cancer cells.

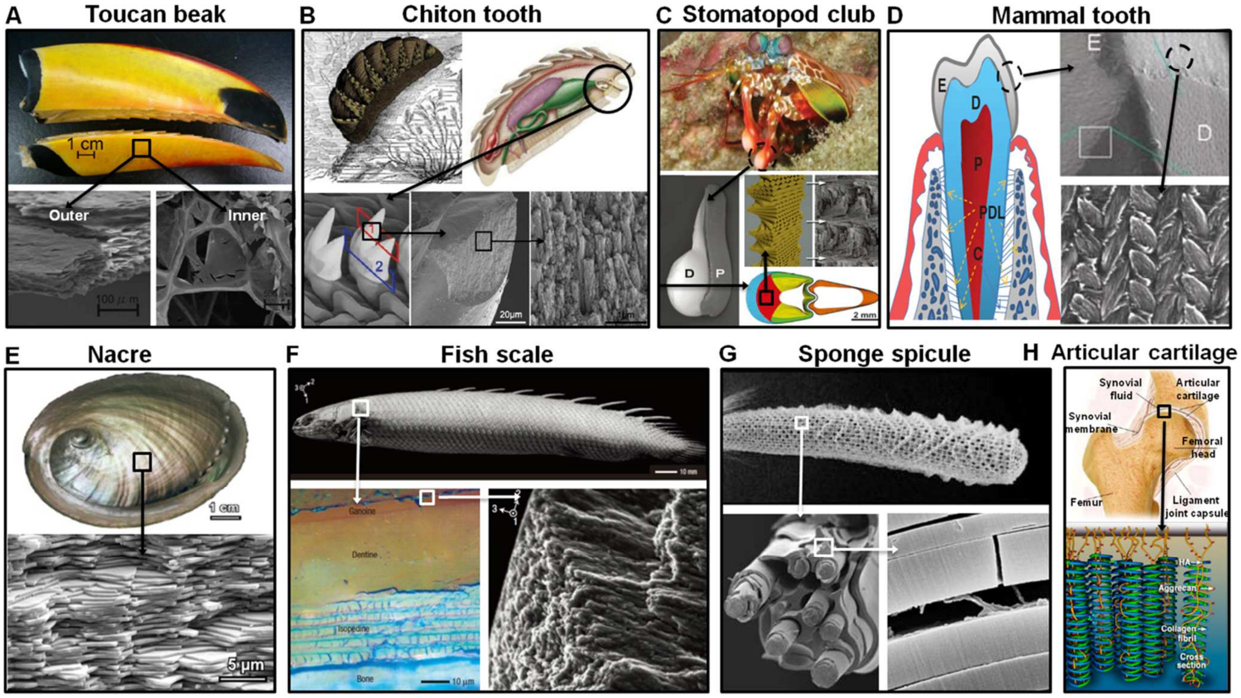

Fig. 1 The macroscale images and corresponding micro/nano structures of natural abrasion-resistant materials. (A) The toucan beak can be utilized for feeding purposes, which consists of the exterior shell based on overlapped keratin scales connected by glues. (B) Chiton radular tooth with closely packed magnetite rod-like ultrastructure is used for grazing algae from rocky surfaces. (C) Stomatopod dactyl club has chitin fiber-based twisted structures for reducing external impaction when smashing the highly mineralized shell of prey. (D) Mammalian enamel is used for cutting and chewing foods, which owns woven rod-based structures composed of hydroxyapatite. (E) The layer-like nacre of gastropod assembled by micrometer scaled aragonite platelets protects its inner soft body. (F) The fish scales can be used for preventing the attack from their predators, which have rod-like, pseudo-prismatic crystallites of apatite in its ganoine layer. (G) Glass sponge is used to support entire structure from fracture, exhibiting a fiber-reinforced composite structure with silica spicules bundles embedded in a layered silica matrix. (H) Articular cartilage can be used for locomotion, where the mechanically trapped complex of hyaluronic acid and lubricin can be used for the reduction of the friction force and the elimination of wear damage to the rubbing/shearing surfaces. (A) Adapted from ref. 4 Copyright 2005, Elsevier Ltd. (B) Adapted from ref. 5 Copyright 2010, Elsevier Ltd. (C) Adapted from ref. 6 Copyright 2012, Science. (D) Adapted from ref. 7 Copyright 2008, Materials Research Society. (E) Adapted from ref. 8 Copyright 2011, Elsevier B.V. (F) Adapted from ref. 9 Copyright 2008, Macmillan Publishers Limited. (G). Adapted from ref. 10 Copyright 2005, American Association for the Advancement of Science. (H) Adapted from ref. 11 Copyright 2011, The National Academy of Sciences of the USA.

Shutao Wang

Shutao Wang is currently a full professor at TIPCCAS. He received his B.S. degree (2000) and M.S. degree (2003) from Northeast Normal University and his Ph.D. degree in 2007 from ICCAS under the supervision of Prof. Lei Jiang. Then he worked in Department of Molecular & Medical Pharmacology and California NanoSystem Institute at University of California at Los Angeles, as a postdoctoral researcher (2007-2010). He was appointed as a full Professor of Chemistry in 2010-2014 at ICCAS. His research interests include the design and synthesis of bio-inspired interfacial materials with special adhesion and their applications at the nano-biointerface.

e.g., bullet proof vest with lightweight and highly flexibility. Therefore, great effort should be devoted to exploring new design principles and strategies of abrasion-resistant materials.

With the long term evolutions, nature creates countless mysterious livings with perfect performance to adapt their surrounding environments (*e.g.*, predator and external pressure). Inspired by these natural examples, a large amount of bio-inspired materials with outstanding physicochemical properties have been fabricated to fulfill special demands such as superhydrophobic surfaces with self-cleaning property inspired by lotus leaves, photonic crystal arrays with structural color inspired by peacock feathers, and nano-biointerfaces with specific recognition to cancer cells inspired by immune system. These successful studies enlighten us to look for new insights from nature to develop more bio-inspired functional materials.[3] To obtain excellent abrasion-resistant performance along with some special features (*e.g.*, lightweight), bio-inspired abrasion-resistant materials are designed

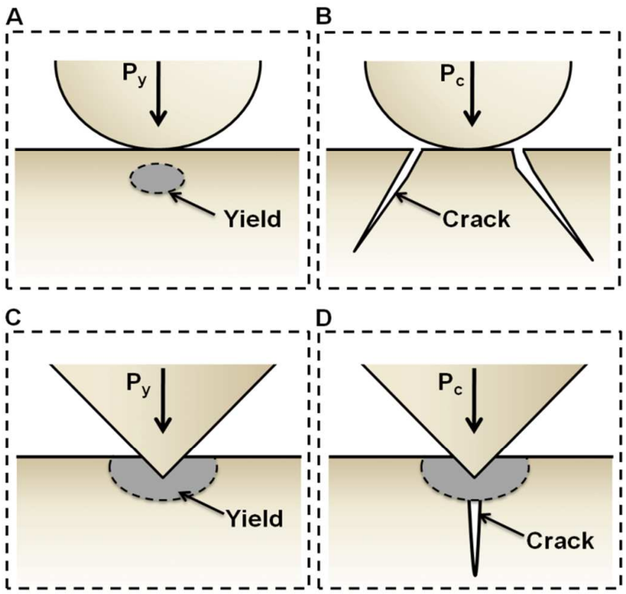

Fig. 2 The schematic view of damage mechanisms at contacts between an elastic indenter and a flat biological material. (A) Yielding damage beneath a blunt contact. (B) Cracking damage at a blunt contact. (C) Yielding damage at a sharp contact. (D) Cracking damage at a sharp contact. Due to limited data available for biological materials, the influence of friction is not considered here. Adapted from ref. 16 Copyright 2013, Elsevier Ltd.

and developed by employing design principles of natural materials with various biofunctions of abrasion resistance, including biotools for feeding purposes, protective armors for preventing predators attack, and supporting materials for supporting body and/or locomotion. For feeding purposes, the exterior shell of toucan beak is found for feeding foods, where their overlapped keratin scales connected by glues (Fig. 1A).[4] Chiton radular tooth with closely packed magnetite rod-like structures is used for grazing algae from rocky surfaces (Fig. 1B).[5] Stomatopod dactyl club is used for smashing the highly mineralized shell of prey, where the helicoidal structural motif of chitin fibril (named Bouligand) is designed for mitigating impaction (Fig. 1C).[6] Mammalian enamel can cut and chew foods, owing to their woven structures of hydroxyapatite rod (Fig. 1D).[7] For protective purposes, the nacre of gastropod can protect its inner soft body from predators attack and external harsh environments (*e.g.*, high pressure), due to its layer-like structures assembled by microscaled aragonite platelets (Fig. 1E).[8] The scales of *Polypterus Senegalu* (*P. Senegalu*, a kind of ancient fish), which have rod-like, pseudo-prismatic crystallites of apatite in its ganoine layer, can prevent themselves from the attacking of their predators (Fig. 1F).[9] For supporting and moving purposes, glass sponge (*Euplectella sp.*) can support entire structure from fracture during impaction events from sea water, due to their fiber-reinforced composite structure with silica spicules bundles embedded in a layered silica matrix (Fig. 1G).[10] Articular cartilage can be used for locomotion, where the complex of hyaluronic acid and lubricin can be employed as an effective lubricant for reducing the friction force and eliminating wear damage to the surfaces (Fig. 1H).[11] Therefore, it may provide novel and ingenious ideas to guide the design and synthesis of bio-inspired abrasion-resistant materials by mimicking natural materials with unique abrasion-resistant biofunctions from their chemical components and exquisite micro/nano-structures.

As there have been several high-quality reviews and books about the exploration of natural abrasion-resistant materials mainly based on lubricating materials and mechanisms such as cartilage and joints, this review will not include them.[1, 12] In this tutorial review, we will summarize the recent progress of natural and bio-inspired materials with outstanding abrasion-resistant property. Firstly, we will briefly introduce the theoretical basis of anti-abrasion and related ranking parameters of natural abrasion-resistant materials. Then, the relationship between chemical components, multiscale micro/nano structures and their unique abrasion-resistant properties are summarized to unravel the possible design principles of natural abrasion-resistant materials. Next, several bio-inspired abrasion-resistant materials based on natural design principles are also presented. Finally, future challenges and opportunities of designing artificial abrasion-resistant materials will be also discussed in this tutorial review.

2. The theoretical basis for assessing abrasion resistance

In classical theories of abrasion, hardness (H) is usually regarded as the primary mechanical property for assessing abrasion-resistant performance of hard materials, which generally have a high elastic modulus (E).[13] Generally, the higher H value represents better abrasion resistance. However, soft polymeric materials with lower H value also provide excellent abrasion resistance in impact and erosion conditions which may result from their extremely low E value. The ranking parameter H/E ratio is proposed to take place of H for preferably predicting abrasion resistance of materials. In recent years, a modified H/E (*i.e.*, $H^{3/2}/E$) has been employed to assess abrasion resistance of natural materials (*e.g.*, *Nereis* jaws).[1, 14] The higher value of $H^{3/2}/E$ probably implies their better abrasion resistance, which is fit for experimental results. However, single criterion isn't always fit for sophisticated abrasion processes, probably eliciting improper or wrong conclusions. Therefore, proper ranking parameters should be adopted according to their respective abrasion mechanisms.

2.1 Abrasion mechanisms

Generally, friction plays a crucial role in the abrasion-resistant performance of engineering materials (*e.g.*, SiC and PMMA).[15] However, because of the limited data available for natural materials, scientists often neglect this aspect and mainly focus on the irreversible contact damages.[16] To simplify research models, natural and abrasive materials can be firstly regarded as flat plates and indenter with the radius of curvature (R), respectively. Then, two limiting contact modes between natural and abrasive materials are proposed including blunt contacts with and sharp contacts, where the contact circle radius (a) is far less than R in blunt contacts and R is close to 0 in sharp contacts. Furthermore, two failure events are considered such as yielding (*i.e.*, plastic deformation) and cracking damage (*i.e.*, fracture damage), where P_y and P_c represent a critical normal pressure for yielding and cracking damage, respectively. Based on above-mentioned considerations, four idealized abrasion scenarios and corresponding equations of abrasion mechanisms are created and shown in the following parts (Fig. 2).

(i) Yielding damage at a blunt contact (Fig. 2a):

$$P_y/R^2 = C_1\left(H^3/\bar{E}^2\right)(1+\bar{E}/\bar{E}')^2 \quad (1)$$

Where $\bar{E}$ and $\bar{E}'$ are the plane-strain modulus of the abraded and abrasive material, respectively. The C_1 is about 0.8. $\bar{E} = E/(1-\nu^2)$ where v is the Poisson's ratio (ca. 0.3 in all cases).

(ii) Cracking damage at a blunt contact (Fig. 2b):

$$P_c/R^2 = C_2(G_c/R)(1+\bar{E}/\bar{E}') \quad (2)$$

Where C_2 is a constant obtained by experimental calibration. G_c is the critical energy release rate (fracture energy), which can be obtained from the equation $G_c = K_{Ic}^2/\bar{E}$. K_{Ic} is fracture toughness.

(iii) Yielding damage at a sharp contact (Fig. 2c):

$$P_y/h_r^2 \approx C_3 H \quad (3)$$

Where h_r is a prescribed residual penetration depth after contact and C_3 is a constant that depends on the projected area of contact.

(iv) Cracking damage at a sharp contact (Fig. 2d):

$$P_c \approx C_4 K_{Ic}^4/H^3 \quad (4)$$

Where C_4 represents a calibration constant depending on the contact geometry, and is obtained through experimental results.

Therefore, intrinsic mechanical properties of natural materials such as H, E and K_{Ic} play a crucial role in affecting their abrasion-resistant performance.

2.2 The ranking parameters for assessing abrasion resistance

Based on these equations, abrasion-resistant performance of natural materials can be verified and further compared through related ranking parameters. For instance, in equations (1), the yielding load (P_y) from a blunt contact is governed by the property parameter $H^3/\bar{E}^2$ times an elastic mismatch parameter $\left(1+\bar{E}/\bar{E}'\right)^2$. When the stiffness of the abrasive materials is infinite (*i.e.*, $\bar{E}' >> \bar{E}$), the value of $\left(1+\bar{E}/\bar{E}'\right)^2$ is close to 1. Therefore, the abrasion-resistant performance of natural materials can be quickly predicted by comparing the ranking parameter $H^3/\bar{E}^2$ or its adapted H^3/E^2.

Similar to equation (1), the other three abrasion equations further reveal that abrasion-resistant performance of natural materials can be dominated by the ranking parameters $K_{Ic}^2/\bar{E}$ or (K_{Ic}^2/E) for equation (2), H for equation (3) and K_{Ic}^4/H^3 for equation (4), respectively. For instance, fracture toughness (K_{Ic}) dramatically influences the abrasion resistance of natural materials with the ranking parameter of K_{Ic}^4/H^3 (Fig. 3). It could be also found that heavily mineralized materials, owing to their generally lower K_{Ic} values, appear to be more prone to abrasion damage from sharp contact. However, mineralized structures with high K_{Ic} values (*e.g.*, nacre) can compete with some weakly mineralized materials. In addition, a adapted ranking parameter $K_{Ic}^4/H \cdot E^2$ can also be utilized for assessing the fracture resistance of sponge biosilica.[17] Therefore, appropriate ranking parameters should be employed for accurately accessing abrasion-resistant performance of materials and guiding the selection of natural models.

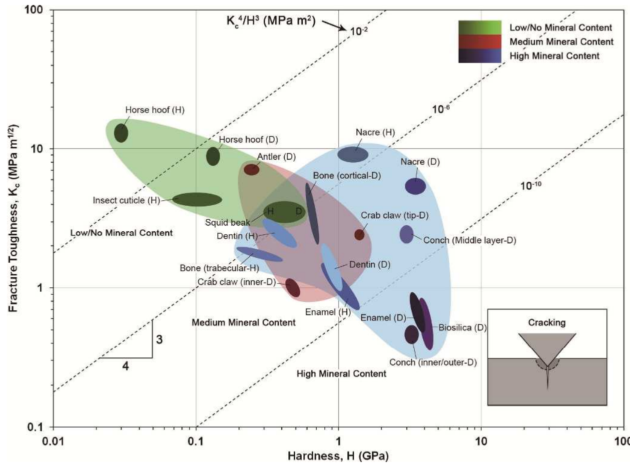

Fig. 3 Selection chart of biological materials for resistance against cracking during a sharp contact. Adapted from Ref. 16 Copyright 2013, Elsevier Ltd.

2.3 Characterization methods

To design bio-inspired abrasion-resistant materials, natural design principles should be pre-explored by employing proper characterization methods. On one hand, H and E can be assessed by nanoindentation experiments and thus calculated from the load-displacement curves following Oliver and Pharr method.[18] While K_{Ic} can be measured by carrying out single-edge notched beam (SENB) tests.[19] When obtaining these mechanical properties (*i.e.*, H, E and K_{Ic}), it is easy to assess abrasion-resistant properties of natural materials by directly comparing these ranking parameters. On the other hand, the crucial role of chemical components can be further disclosed by integrating indentation data with the results of modern characterization technologies such as energy dispersive X-ray spectroscopy (EDX), microbeam scanning wide-angle X-ray scattering (WAXS) measurements and Raman imaging. For example, EDX maps can verify the spatial distribution of elements such as Zn (red), Ca (blue) and Cl (green) in the fang of a spider (Fig. 4A), revealing correlation between the $H^{3/2}/E$ ratio and Zn/Cl enrichment.[20] By means of WAXS measurements, the micro-diffractograms of a crayfish molar tooth provide mineralogical identification, relative abundance and orientation information in Fig. 4B.[21] A two-dimensional (2D) Raman image of byssus thread cuticle (*M. californianus*) can be used to distinguish the intensity and distribution of the Fe-dopa crosslinking, disclosing that granule parts have higher crosslinking intensity than matrix (Fig. 4C).[22] In addition, it is also easy to reveal the relationship of these mechanical properties and micro/nano structures by integrating indentation results and microscopy technologies such as optical microscopy, scanning electron microscopy (SEM) and transmission electron microscopy (TEM). For example, the optical images of the dactyl club from dark field (DF), bright field (BF), and differential interference contrast (DIC), show the locations of the impact and periodic region (Fig. 4D).[6] The SEM images of the fracture tooth tip of a sea urchin show that single crystal needles embedded in a polycrystalline matrix, which owns higher modulus and hardness values (Fig. 4E).[23] The TEM images of a *Glycera* jaw tip show mineralized fibers are embedded in a protein matrix (Fig. 4F).[24]

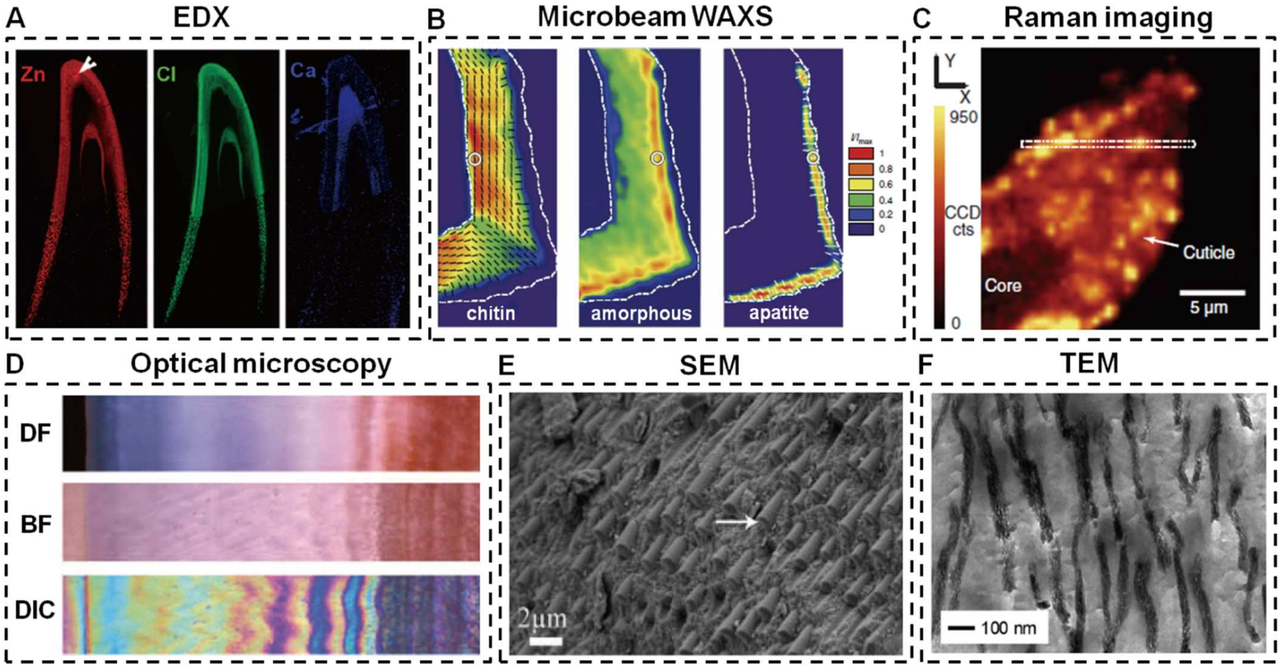

Fig. 4 (A) The Zn, Cl and Ca distribution maps of the spider's fang from EDX measurements. (B) The synchrotron scanning WAXS measurements of the crayfish molar tooth reveal the distribution of chitin and apatite. (C) 2D Raman image of byssus cuticle reveals that granules have higher Fe-dopa intensity than matrix. (D) The optical images indicate the locations of the impact and periodic region in the dactyl club. (E) SEM images of the fracture tooth tip of a sea urchin show the single crystal needles (white arrow) embedded in a polycrystalline matrix. (F) TEM images of thin sections of a *Glycera jaw tip show* mineralized fibers (dark) are embedded in a protein matrix (light gray). (A) Adapted from ref. 20 Copyright 2012, WILEY-VCH Verlag GmbH & Co. KGaA, Weinheim. (B) Adapted from ref. 21 Copyright 2012, Macmillan Publishers Limited. (C) Adapted from ref. 22 Copyright 2010, American Association for the Advancement of Science. (D) Adapted from ref. 6 Copyright 2012, American Association for the Advancement of Science. (E) Adapted from ref. 23 Copyright 2008, WILEY-VCH Verlag GmbH & Co. KGaA, Weinheim. (F) Adapted from ref. 24 Copyright 2007, The National Academy of Sciences of the USA.

The indention results also reveal that the minor role of atacamite fibers in improving hardness and modulus. Therefore, the effective combination of indentation results with these characterization methods provides a promising route to clarify the influence of chemical components and micro/nano structures on mechanical properties and relevant abrasion-resistant properties. Therefore, we will introduce the design principles of natural abrasion-resistant materials from the aspects of chemical components and micro/nano structures in the following parts.

3. Chemical design of abrasion-resistant materials in nature

Commonly, abrasion-resistant properties of natural materials can be rendered by employing limited chemical components such as minerals, proteins and polysaccharides. In addition, a few metal ions (*e.g.*, Zn^{2+}) can be used as cross-linkers to form metal complexes with specific proteins, thereby enhancing the hardness and stiffness of natural materials (*e.g.*, *Nereis* jaws).[14, 25] Therefore, we will discuss the chemical design of natural abrasion-resistant materials from three following categories: minerals (*e.g.*, hydroxyapatite, calcium carbonate, magnetite and gregite), metal ions (*e.g.*, Zn^{2+} and Fe^{3+}), and organic components including proteins (*e.g.*, keratin and collagen) and polysaccharides (*e.g.*, chitin).

3.1 Mineral components

Hydroxyapatite (HA) and its derivatives are the predominant minerals in many natural abrasion-resistant materials such as mammal teeth and the osteoderms of alligator and armadillos.[26-29] As well known, HA shows a hexagonal structure ($P6_3$/m) with the formula of $Ca_{10}(PO_4)_6(OH)_2$ (Fig. 5A).[30] Because of an abundance of substitutions and vacancies, the molar ratios of Ca/P can be varied from the ideal value (1.67) in biomineralized tissues and some derivatives are commonly adopted for special functions. For example, fluorapatite ($Ca_{10}(PO_4)_6F_2$) is employed by teeth for enhancing hardness and reducing acid corrosion.

Calcium carbonate ($CaCO_3$) is commonly found in tissues of natural organisms by employing different polymorphs such as calcite (rhombehedral), aragonite (orthorhombic), and amorphous calcium carbonate (ACC) in Fig. 5A.[30] For example, the shells of bivalve *Placuna placenta* (*P. placenta*) are composed of calcite which is 50% harder than pure calcite.[31] In sea urchin teeth, calcite matrix with high content of Mg (40-45%) forms a misoriented polycrystalline structure, which is stronger and harder than single crystalline needles and plates of calcite with low content of Mg (4.5-

13%).[23] The nacreous layers of gastropods are usually aragonite.[8] While, the ACC form is found in the cuticles of crustacean (*e.g.*, lobster and crab) and mandibles of the freshwater crayfish.[21, 32]

Silica is usually found in the form of amorphous, hydrated $SiO_2 \cdot nH_2O$ in the beautiful and intricate skeletons of the most ubiquitous diatoms in the oceans. In the sea water, there are more calcium elements (ca. 400 ppm) than silicon (ca. 3 ppm). But why not calcium but silicon-containing minerals are formed in diatoms? This interesting phenomenon can probably be explained from two aspects: mechanical enhancement and energetic issue. On one hand, tensile fracture stress of a diatom (*e.g.*, *Fragilariopsis kerguelensis*) frustules at 540 N mm^{-2} is much higher than that of aragonite ($CaCO_3$) at 100 N mm^{-2}. This implies that diatoms fabricated from $SiO_2 \cdot nH_2O$ are more mechanically robust than that fabricated from $CaCO_3$.[33] On the other hand, the transportation of silicic acid through diffusion and subsequent silica auto-polymerization through organics catalysis (*e.g.*, silaffins and long-chain polyamines) both required less energy.[30] On the contrary, aggregation of calcium carbonate in their supersaturated solution and their relocation in cell interior need additional energy. Therefore, silica rather than calcium carbonate are employed for the skeletons of marine diatoms.

Different from these typical biominerals, some other ones (*i.e.*, magnetite and gregite) are also employed for improving abrasion resistance of natural materials. For example, the veneer part of chiton radular teeth is composed of magnetite (Fe_3O_4) in Fig. 5A, which exhibit three times higher hardness than that of enamel and nacre, resulting in unexpected abrasion-resistant capability for repeatedly scraping off nutrients from rocks.[5] More interestingly, the distinct gradient in mechanical properties can be produced by further integrating a softer mineral layers of lepidocrocite (γ-FeO(OH)) in the interior of chiton radular teeth. This unique design strategy endows the radular teeth with a specific self-sharpening feature. In addition, mineral gregite (Fe_3S_4) is newly discovered in the outer layer of gastropod mollusc shell (*Crysomallon squamiferum*, *C. squamiferum*), which live in deep-sea hydrothermal vent with high temperature, high pressures and high concentrations of sulfides.[34] Although the outer gregite layer is softer than inner aragonite layer, it is still regarded as the first line of defense against a penetrating impact from predators.

3.2 Metal ions

To obtain appropriate abrasion resistance, metal ions such as (Zn^{2+} and Fe^{3+}) are employed to improve mechanical properties (*e.g.*, hardness and stiffness) of natural materials by forming metal-protein cross-linking. Therefore, multiple biofunctions can be further realized such as biotools for catching preys and cuticles for protecting internal soft body (Fig. 5B).[25]

In recent years, Lichtenegger and his coworkers have reported that by the coordination of Zn^{2+} and nitrogen atoms in the imidazole rings of histine protein (His), Zn-His cross-linking is employed to promote the abrasion-resistant feature of *Nereis* jaws (Fig. 5B, top).[14] The contribution of Zn^{2+} cations to the mechanical properties of jaws can be revealed by the combination of X-ray absorption images for Zn^{2+} distribution and indentation results for the hardness and modulus. When removing Zn^{2+} from jaw samples, significant reductions of mechanical properties (*i.e.*, *H* and *E*) can be clearly observed. By soaking samples in a Zn^{2+} cations enriched solution, the lost mechanical properties can be almost regained which may come from the re-introduction of Zn. These experimental results demonstrate that the Zn-His cross-linking interaction is critical for the hardness and modulus of jaws.

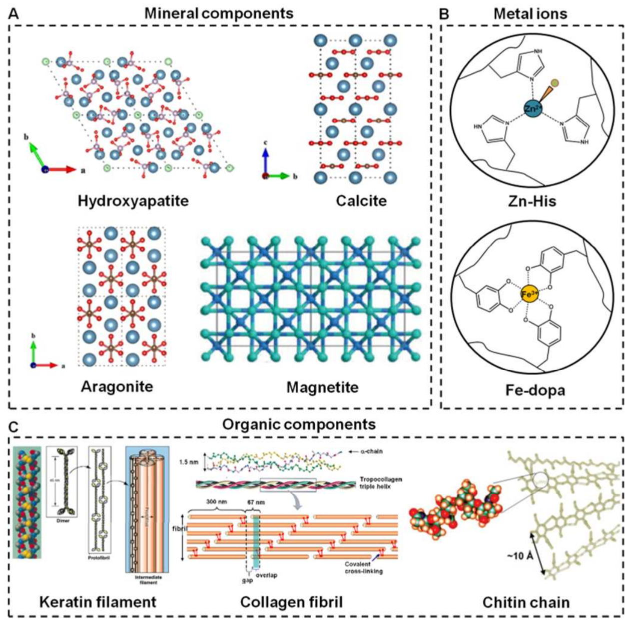

Fig. 5 The chemical components commonly used for the construction of natural abrasion-resistant materials. (A) The mineral components such as hydroxyapatite, calcite, aragonite and magnetite. (B) The metal ions used for metal-protein crosslinking interaction such as Zn-His and Fe-dopa. (C) Organic components such as keratin filament, collagen fibirl and chitin chain. (A) Adapted from ref. 30 Copyright 2012, Elsevier Ltd. Adapted from ref. 5 Copyright 2010, Elsevier Ltd. (B) Adapted from ref. 25 Copyright 2014, Wiley-VCH Verlag GmbH & Co. KGaA, Weinheim. (C) Adapted from ref. 30 Copyright 2012, Elsevier Ltd. Adapted from ref. 39 Copyright 2010, WILEY-VCH Verlag GmbH & Co. KGaA, Weinheim.

Harrington *et al.* have revealed that hardness can be promoted in the example of the mussel byssus cuticle, resulting from the increased cross-linking density between Fe ions and dopa (3,4-dihydroxyphenylalanine) (Fig. 5B, bottom).[22] The 2D Raman imaging in Fig. 4C shows that the granular part of the cuticle has much higher Fe-dopa cross-link density than surrounding matrix. Similar to Zn-His cross-linking,[14] the key role of Fe-dopa cross-linking for improving hardness of cuticle can also be revealed by the experimental results of EDTA treatment. Furthermore, a higher extensibility is observed in the less cross-linked matrix portion of cuticles.

3.3 Organic components

Different from the hardness enhancement of minerals and metal ions, the organic components such as proteins (*e.g.*, keratin and collagen) and polysaccharides (*e.g.*, chitin) are often softer and tougher materials, which can be widely employed as buffer layers for resisting load impaction and/or adhesive layers for resisting fracture.

Keratins are composed of two α-helices bundling into a superhelix coiled-coil, gradually assembling into intermediate filament (Fig. 5C, left). The vertebrates (*e.g.*, alligators and armadillos) commonly consists of a strong exoskeleton coated by a softer and tougher keratin layer, which is similar to the protective design in the turtle shell.[35] For example, turtles have evolved robust, boney shells covered by thin keratinous wavy multi-layers, termed scutes. Although its contribution to resist quasi-static flexural loads was found to be negligible, a remarkable toughening effect was observed by comparing impact toughness from keratin samples and keratin peeled samples.

Collagen is the most abundant protein in fish scales, armadillo amours and turtle carapaces. Collagen molecule frequently has the defining amino acid sequence of Gly-Pro-X or Gly-X-Hyp (Gly = glycine, Pro = proline, Hyp = hydroxyproline, X = other amino acids). The tropocollagen molecules are formed from the combination of three α-helix strands of the collagen molecule. The as-prepared tropocollagen triple helix can be used to generate collagen fibrils (Fig. 5C, middle). Collagen is usually in the mineralized or non-mineralized forms for different biological goals. For example, the mineralized collagen fibrils can be used for assembling Bouligand-type arrangement in the scales of *Arapaima gigas* (*A. gigas*), endowing their unique protective properties.[36] Different from the fish scales, non-mineralized collagen fibers in armadillo armors and turtles carapaces can be employed for connecting the tiles or boney ribs together, thereby providing flexibility.[29, 37]

As the second most abundant organic material on earth, chitin is a polysaccharide which is often found in the insects and exoskeletons of crustaceans.[38-40] To provide excellent mechanical properties for abrasion resistance, chitin can be used to assemble hierarchical structures by employing three kinds of polymorphic forms (*i.e.*, α-chitin, β-chitin and γ-chitin). For example, the crystalline α-chitin usually predominates in the exoskeleton of large crustaceans, where the sugar residues are heavily H-bonded imparting stiffness and chemical stability (Fig. 5C, right),[39] which are individually wrapped by proteins. However, it is difficult to work with chitin because of its low solubility. Therefore, chitosan, as the more soluble and highly deacetylated form of chitin, has commonly been used for fabricating artificial materials with high strength toughness.[41]

4. Structural design of abrasion-resistant materials in nature

Although natural materials take advantage of limited chemical compositions, they still exhibit promising abrasion-resistant features which may mainly lie in their exquisite structural design with the dimensions varying from the nanoscale to the macroscale. However, these multiscale structures in nature are extremely complex and elusive, resulting in the uncertainty of their structural design principles and abrasion-resistant features. To provide a basic guidance of bio-inspired abrasion-resistant materials, we here try to understand structural design principles from three following parts: i) introduce fundamental building units including particles, platelets, rods, fibers and pores for disclosing their roles in abrasion resistance; ii) explain multiscale structures by the integration of these structural units, generating two representative multilayer structures (i.e., hard exterior-soft interior and hard interior-soft exterior); iii) employ computational simulations for further revealing advantages of structural design such as stress redistribution and energy dissipation.

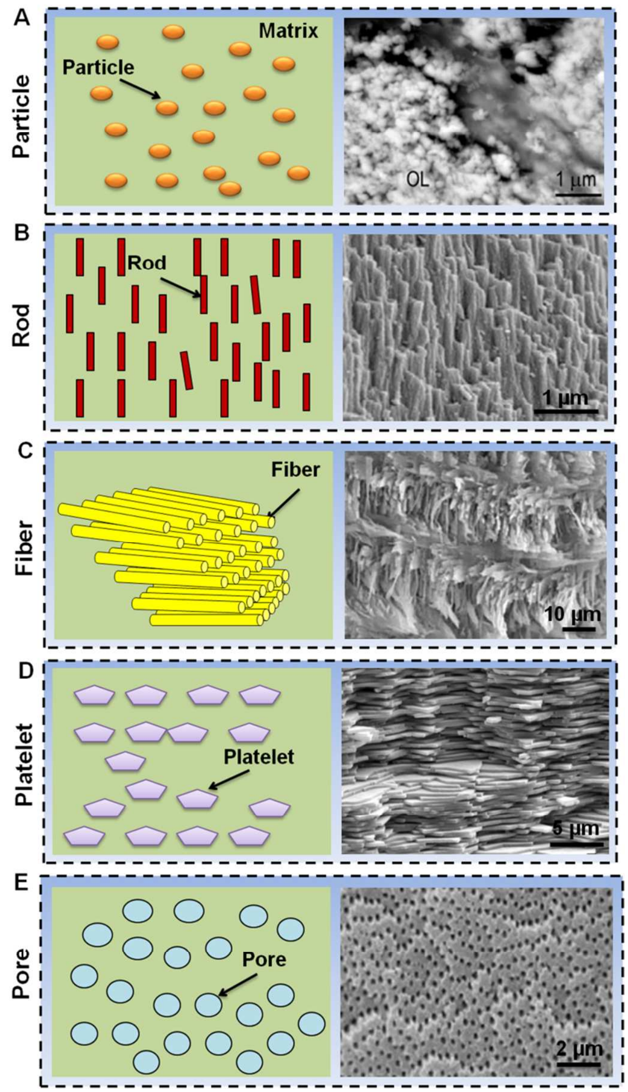

Fig. 6 The fundamental structural units employed in natural materials for providing mechanical properties. (A) particle-based composite structure from the shell of a gastropod mollusc. (B) rod-based composite structure from the veneer of chiton teeth. (C) Fiber-based composite structure from the exoskeleton of lobster. (D) Platelet-based layer structure from nacre. (E) Nanoporous structures from sucker ring teeth of Humboldt squid. (A) Adapted from ref. 34 Copyright 2010, The National Academy of Sciences of the USA. (B) Adapted from ref. 7 Copyright 2010, Elsevier Ltd. (C) Adapted from ref. 39 Copyright 2010, WILEY-VCH Verlag GmbH & Co. KGaA, Weinheim. (D) Adapted from ref. 42 Copyright 2011, Elsevier B.V. (E) Adapted from ref. 44 Copyright 2009, WILEY-VCH Verlag GmbH & Co. KGaA, Weinheim.

4.1 Fundamental building units

4.1.1 Particles. Particles (*i.e.*, granules) as zero-dimensional (0D) building units are found in different forms such as minerals and cross-linking compounds.[22, 34] For example, the outermost layer (OL) of *C. squamiferum* shell exhibits a nanoparticle-based composite structure composed of mineral gregite particles with diameter down to about 20 nm and organic components (Fig. 6A).[34] Although outer gregite layer is softer than inner aragonite layer, it is still considered as the first line of defense against a penetrating impact event. Furthermore, deformation mechanisms are successful proved by the load applied perpendicular to the top surface of shell in Vickers microhardness experiments. The granular structure is clearly observed to consolidate within and around the indent. More importantly, the separation of granules results in tortuous and noncontinuous microfractures, as well as jagged crack fronts, which promote energy dissipation and thereby prevent catastrophic brittle fracture.

4.1.2 Rods. Rods regarded as one-dimensional (1D) rigid building units for the construction of multiscale micro/nano structures for tolerating abrasion. They can be usually found in many natural abrasion-resistant materials in the form of hard minerals such as enamel parts of mammal teeth, ganoine layer of ancient fish scales and veneer of chiton radular teeth.[5, 7, 9] For example, the veneer of chiton teeth consists of the rod-like magnetite crystallites which are surrounded by a thin chitin layer in Fig. 6B.[5] The magnetite veneer has a modulus ranging from 90 to 125 GPa and a corresponding hardness ranging from 9 to 12 GPa. To the best of our knowledge, these values represent the highest modulus yet reported for a biomineral. By comparing the value of H^3/E^2, the chiton teeth exhibit better performance against abrasion than the hardest biominerals: enamel and nacre, where the abrasion mechanism is limited to the yielding damage in a blunt contact. When changing to cracking event by sharp stiff particles, it can be accessed by the ratio of $\boldsymbol{K_{\mathrm{Ic}}^4/H^3}$ or $\boldsymbol{K_{\mathrm{Ic}}^4/H\cdot E^2}$.[17] Hence, a moderate increment of fracture toughness significantly improves the abrasion resistance. Their anisotropic rod-like substructure provides the design cues that could be used in the fabrication of ultrahard materials with outstanding abrasion-resistant properties.

4.1.3 Fibers. Fibers as 1D soft building units are usually found in fish scales and crustacean cuticles which are composed of mainly softer organic components (*e.g.*, chitin or collagen) and employed for resisting external load and enhancing energy dissipation.[6, 36, 38] For example, the cuticle of the lobster (*Homarus americanus*) consists of chitin-protein fibers embedded in a mineral-protein matrix.[39] The chitin-protein fibers reinforce the cuticle and further assemble twisted plywood (Bouligand-type arrangement, Fig. 6C) which not only resist macroscopic loads, but also dissipate significant amounts of energy during impact processes. When moving from nanoscale to macroscale, the anisotropy ratios vary from 4.25 for single-crystalline chitin, to 1.75 for mineralized chitin-protein nanofibrils, and down to 1.4 for twisted plywood structures without pore canals. The efficient reduction in anisotropy increases significantly the cuticle stiffness along its normal direction. Therefore, twisted plywood composites, where each layer is reinforced with soft polymer coated high-modulus fibers, could be used for structural and armor applications.

4.1.4 Platelets. Platelets as two-dimensional (2D) building units are usually found in the nacreous layer of some mollusk shells (*e.g.*, gastropod and bivalve).[42] For example, the nacre from red abalone (*Haliotis rufescens*) exhibits the famous "brick-and-mortar" structure with polygonal shaped platelets as bricks and the organic matrix as mortars in Fig. 6D. The aragonite platelets take over about 95 wt% of the nacre with the diameter of 5-20 μm and thickness of 0.3-1.5 μm, depending on different species. The surface of platelets in nacre is pretty rough and corrugated, showing nanoscale asperities. The high local stiffness and strength of the individual nacre platelets suggested that the platelets can serve as the primary load-bearing elements facilitating energy dissipating mechanisms. In addition, it has also been suggested that nanoasperities interacting and mechanical interlocking occurred on the platelets surface provide resistance to interfacial sliding, thus promoting fracture resistance.

4.1.5 Pores. The three-dimensional (3D) building units, pores, can be generally found in many natural materials such as diatoms, sponges, and turtle shells, as well as toucan beak, for resisting impaction and fracture and/or reducing weight of natural materials.[4, 10, 35, 43] For example, the sucker ring teeth of squid consist of relatively uniform local pores and highly parallel nature of the fused tubular (Fig. 6E), which is well suited to penetrate the skin or scales of prey.[44] The pore diameter increases gradually from around 100 nm close to the surface and reaches over 99% of the maximum values (259 nm) at a distance from the surface equivalent to approximately 20% of the tooth diameter. The orientation of the pores that run parallel to the long axis of the teeth probably increase their bending stiffness, a feature that is most important where they are likely to be subjected to large bending or shear forces, because the suckers themselves are soft actuators that flex in many directions. In addition, the graded hardness (*i.e.*, harder at the tooth edge, and gradually softer towards the tooth interior) resulting from the porosity gradient is a micromechanical feature recently observed in several structural materials from nature that exhibit a high abrasion tolerance due to their direct contact with the external environment.

4.2 Multilayer design principles

Natural materials have arisen over long terms of time and consist of abundant exquisite design principles.[45] However, monolithic structures are rarely employed in these natural designs. On the contrary, multiscale systems, especially for multilayer design, are extremely preferred and often employed by natural abrasion-resistant materials, thereby endowing their promising impaction and penetration resistance along with unique features such as lightweight and flexibility. In the following parts, we will discuss two representative examples with multilayer designs including multilayer materials with hard exterior and soft interior, and multilayer materials with soft exterior and hard interior.

4.2.1 Multilayer design with hard exterior-soft interior. One of the multilayer design is built from a compliant interior covered by a hard and stiff external layer which is commonly found in natural abrasion-resistant materials such as fish scales,[36] and crab exoskeletons.[46] This structural design endows these materials with desired multi-functionality, resulting in outstanding external penetration resistance without impairing flexibility. For example, *A. gigas* is one of the largest freshwater fish in the world. As illustrated in the top part of Fig. 7A, their scales in adults consist of two

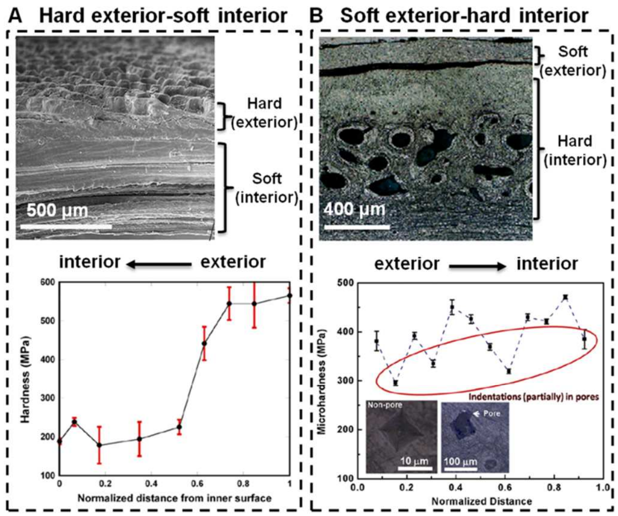

Fig. 7 The typical multilayer structure. (A) The multilayer structure with hard outer and soft inter from scales of fish (*i.e.*, *Arapaima gigas*). (B) The multilayer structure with soft outer and hard inter from shell of armadillos (top) and alligators (bottom). (A) Top adapted from ref. 36 Copyright 2013, Macmillan Publishers Limited. Bottom adapted from ref. 47 Copyright 2011, Elsevier Ltd. (B) Top adapted from ref. 29 Copyright 2011, Elsevier Ltd. Bottom adapted from ref. 27 Copyright 2014, Elsevier B.V.

distinct macro-level layers: a highly mineralized exterior (ca. 600 µm thick) and a lowly mineralized collagen interior employing a Bouligand-type arrangement (ca. 1000 µm thick).[36] The bottom of lamellae can respond to the loading in different directions by reorienting the lamellae, which can be revealed by the combination of mechanical tensile testing and *in situ* SAXS experiments.[36] This enhanced flexibility of the lamellae provides protection to the sophisticated structure of scales by increasing their ductility and toughness to resist their fracture. In addition, the overlapping of the scales allows flexibility through bending of multiple scales. Therefore, this design principle enables natural materials excellent penetration resistance without impairing flexibility. Fig. 7A shows that the hardness of the exterior is over twice that of the internal parts, implying their different functions in the process of predator attack.[47] The highly mineralized outer shell provides hardness to minimize local plasticity and impede the penetration by the predator. While, the Bouligand-type arrangement of the inner

4.2.2 Multilayer design with soft exterior-hard interior. Another representative multilayer design is adopted from harder interior coated by a softer and tougher layer (*e.g.*, keratin) which is found in alligators[27] and armadillos,[29] or presented in toucan beak[4] and turtle shells.[35] For example, *Dasypus novemcinctus* (*D. novemcinctus*) is the most common nine-banded armadillo in the US.[29] Their osteoderms consist of two distinct layers: exterior (*i.e.*, epidermis) and interior (*i.e.*, papillary, reticular and hypodermis) in the top part of Fig. 7B. Similar to armadillos, alligator scute shows a harder interior and softer exterior with zigzag hardness pattern due to the porous structure of alligator scutes (Fig. 7B, bottom).[27] Their epidermis is composed of keratin and plays only a crucial role in waterproof rather than protection against mechanical forces. The bony tiles from interior consist of hard mineralized tiles connected by soft non-mineralized collagen fibrils named Sharpey's fibers. This sandwich tiles endow these animals mobility by reducing low density, whereas Sharpey's fibers connect the tiles together for flexibility. In a live armadillo, these tiles are irrigated by blood and stronger than in the dry condition; the mineralized collagen fibers inside the osteoderms act to impede crack propagation through them, with the Sharpey's fibers ensuring the integrity and toughness of the tiling system. Therefore, this design principle enables natural materials excellent abrasion resistance along with lightweight and flexibility.

4.3 The computational simulation of multilayer structures

Furthermore, multilayered finite element analysis (FEA) computational model and experimental data obtained by indentation experiments are integrated together to disclose the advantages of multilayer structures in an abrasion process. It is benefit for us to understand the effect of many factors on abrasion tolerance such as the individual thickness of a multilayer, the gradients between different layers and stress redistribution during a specific abrasion event (*e.g.*, sharp contact), further revealing the unique design principles of multilayer structures for guiding the design and development of bio-inspired abrasion-resistant materials.

4.3.1 Modeling multilayer design with hard exterior-soft interior. To explain advantages of natural multilayer design with hard exterior and soft interior such as crustacean cuticle and fish scales,[6, 9, 39] the process of predatory attacks are simulated by using multilayered FEA computational model coupled with experimental data. Based on the scales of a fish (*e.g.*, *P. Senegalus*), three kinds of armor models including all-ganoine, discrete and gradient multilayer designs are explored to reveal the advantages of gradient multilayer by comparing their stress and strain contours, and plastic equivalent strain after unloading.[9] The results of computational simulation imply the advantages of several design principles as follows: i) Gradients between layers promote the redistribution of stress. Compared with other two models, the smoother stress distribution in the gradient model in Fig. 8A is believed to reduce interface failure and increase interfacial toughness, thereby improving penetration resistance. As the stiff ganoine transfers load through the ganoine-dentine junction, the underlying softer, more compliant dentine layer dissipates energy via plasticity (at high enough loads). Additionally, the ganoine-dentine junction in *P. senegalus* scales is able to arrest cracks, as in mammalian teeth.[48] ii) Layer thickness should be controlled for reducing weight and controlling cracking mechanism (*e.g.*, ganoine). The thickness of ganoine from 5 to 20 µm promote the advantageous circumferential cracking mechanism through circumferential stress (S22) > radial stress (S11), rather than disadvantageous radial cracking. For a thicker or thinner ganoine layer, S11 remains large, which promote undesirable radial cracking and thus lead to catastrophic failure. iii) Material layer sequence is also critical. For example, reversing the ganoine and dentine layers in a virtual microindentation leads to magnified interfacial tensile normal and shear stresses, promoting delamination. Therefore, the multilayer design with hard exterior and soft interior is suitable for improving fracture and penetration resistance.

4.3.2 Modeling multilayer design with soft exterior-hard interior. On the contrary, the multilayer design with soft exterior and hard interior are also presented in natural abrasion-resistant materials such as alligators,[27] armadillos,[29] toucan beak,[4] and turtle shells[35] as well as shell of gastropod mollusc.[34] Based on the same research method with fish scales of *P. Senegalus*,[9] Ortiz and his coworkers constructed a multilayered model based on shell of a gastropod mollusc (*e.g.*, *C. squamiferum*) and penetrating indent for simulating the loading process of a predatory attack from common Brachyuran crabs.[34] The multilayered shell consist of three layers including the mineralized greigite-based outer layer (OL), organic middle layer (ML), and highly calcified inner shell (IL) composed of gradient layer (GL), and crossed-lamellar layer (CLL). Because the hardness of OL and ML (1.7 and 0.5 GPa) is apparently lower than the IL (5.4 GPa), this structure can be simplified to multilayer design with soft exterior-hard interior. Several safety mechanisms of this multilayer design can be depicted in Fig. 8B as follows: i) Plastic deformation of inner calcified layer (IL) can be remarkably mitigated by the underlying organic ML, demonstrated by comparing inelasticity in the OL and ML from contours of plastic equivalent strain. ii) Resistance to bending and radial displacements is promoted by the rigid IL. If the external load is high enough to penetrate the ML and thus induce plastic deformation of the IL through elevated tensile stresses (*i.e.*, S11, S22, and S33), the IL would be susceptible to fracture normal to the shell surface. If this were to happen, propagating cracks from the IL are arrested by the highly inelastic ML to mitigate catastrophic failure of the shell. Therefore, the multilayer design with hard interior and soft exterior is benefit for promoting the resistance of cracking and penetration through multiple safety mechanisms.

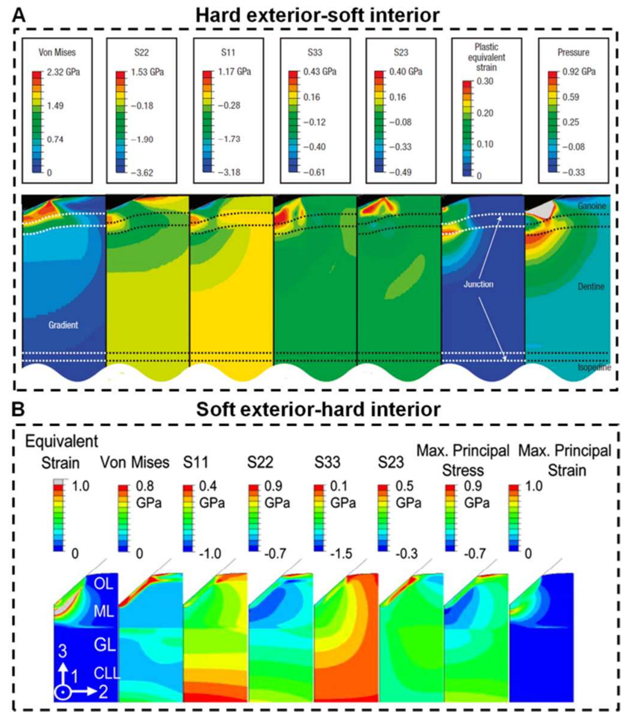

Fig. 8 Computational model of two typical multilayer structures *via* finite element analysis (FEA) simulations, including (A) *P. senegalus* scale with hard exterior-soft interior and (B) Shell of *C. squamiferum* with soft exterior-hard interior. (A) Adapted from ref. 9 Copyright 2008, Macmillan Publishers Limited. (B) Adapted from ref. 34 Copyright 2010, The National Academy of Sciences of the USA.

5. Bio-inspired abrasion-resistant examples

By taking advantage of the explorations of natural abrasion-resistant materials, it is revealed that abrasion resistance is greatly relevant to design principle of chemical components and multiscale micro/nano structures. According to these above mentioned design principles, the artificial examples can be divided into four kinds of abrasion-resistant materials inspired by insect cuticle, nacre, and tooth as well as diatom.

5.1 Insect cuticle inspired abrasion-resistant materials

Inspired by insect cuticle, Ingber and coworkers prepared a laminate composite film called "shrink" which is composed of a layer of protein (*e.g.*, fibroin) and a layer of polysaccharide (*i.e.*, chitosan) (as shown in Fig. 9A).[41] The chemical components of natural cuticle can be mimicked by the combination of fibroin (cuticular structural proteins) and chitosan (a highly deacetylated form of chitin). From the structural point, the shrink composite film shows phased-separated laminar structure which can be extended to multiple shrilk laminates by gluing with fibroin (Fig. 9B). Interestingly, mechanical testing in Fig. 9C revealed that shrilk films exhibit a high strength of 119 MPa, which is ten times stronger than that of a simple mixture of chitosan and fibroin with similar feed ratio, and twice of the strength of single chitosan. In addition, shrilk films also exhibit much higher toughness as it absorbed 1.5 times more energy than chitosan per volume before breaking. This unexpected increase in toughness that allows shrilk films to resist external tension without deforming or damaging internal structural components is similar to the protective function of natural insect are greatly reduced after saturating with water similar to the cuticle features from living insects (Fig. 9D). When coating a protective layer (*e.g.*, parylene-C) for isolating water, shrilk films keep their high strength and shape stability which is similar to the waterproof functions of natural insect epi-cuticle. Therefore, it is a potential strategy to improve the toughness and strength of materials by assembling insect cuticle inspired abrasion-resistant materials.

5.2 Nacre inspired abrasion-resistant materials

Inspired by nacre, ceramic and layered bulk materials with submicrometre layer spacings can be fabricated by taking advantage of ice-templating techniques.[19, 49] For example, Deville and coworkers reported that the nacre-like material exhibits not only an unprecedented toughness for a ceramic material but also a very high strength and stiffness even at high temperature, because it only consists of mineral constituents.[19] This nacre-like material exhibits multilayer structural features, showing closely packed ceramic platelets with surface nano-asperities identical to that of

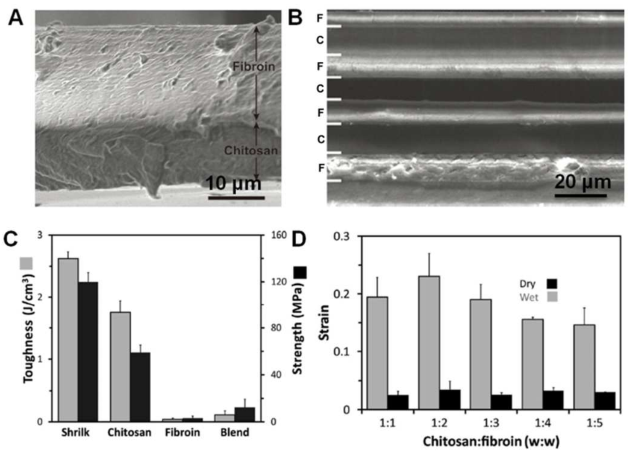

Fig. 9 The multilayer design strategies of bioinspired materials. SEM image of the (A) shrilk laminate and (B) multi-laminate materials. (C) Modulus of toughness (grey bars) and breaking strength (black bars) of the shrilk laminate and other samples. (D) Strain at the break point for shrilk when dry (black bars) compared to when saturated with water (grey bars). Adapted from ref. 41 Copyright 2012, WILEY-VCH Verlag GmbH & Co. KGaA, Weinheim.

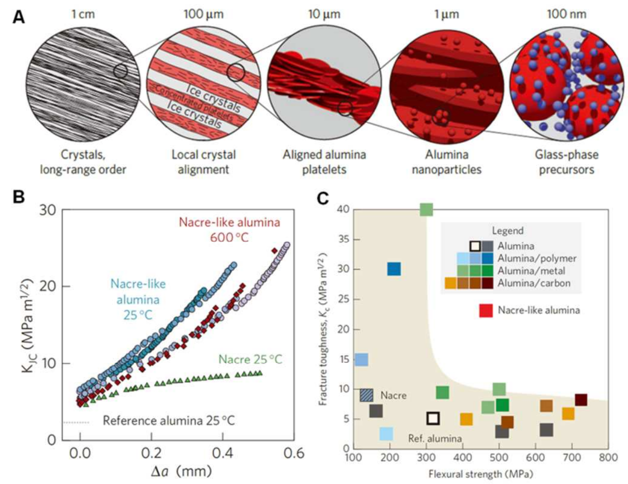

Fig. 10 (A) Self-organization of multilayer structures occurs during the freezing stage. The growth of ordered-ice crystals triggers the local alignment of platelets. Alumina nanoparticles and liquid-phase precursors are entrapped between the platelets. (B) Fracture toughness calculated from the J-integral and crack extension Δa, and the equivalent for nacre-like alumina and nacre. (C) Nacre-like alumina keeps relative higher fracture toughness and flexural strength compared with other reported materials. Adapted from ref. 19 Copyright 2014, Macmillan Publishers Limited.

nacre (Fig. 10A). This nacre-like structure has significantly higher K_{Ic} of 6.2 MPa m$^{1/2}$ than that of polycrystalline alumina (3.5 MPa m$^{1/2}$). Similar to natural nacre, the crack can be deflected by the composite low-stiffness interface and slowed down by various extrinsic toughening mechanisms. This toughening leads to an increase of the fracture resistance as the crack propagates which is known as an *R*-curve effect. Fig. 10B shows that the maximum increase of toughness is ca. 22 MPa m$^{1/2}$ at which corresponds to ca. 350% increase compared to the K_{Ic} toughness and 600% increase compared to the reference alumina. This far exceeds that of nacre and is equivalent to the best brick-and-mortar polymer/ceramic composites developed previously. In addition, nacre-like alumina still owns the higher flexural strength compared with other reported materials (Fig. 10C). Therefore, it is a promising strategy to improve the fracture resistance of materials by designing nacre inspired abrasion-resistant materials.

5.3 Tooth inspired abrasion-resistant materials

In addition to design micro- and nanostructure through self-assembly methods, controlling the orientation and spatial distribution of anisotropic reinforcing particles provide an efficient route for natural materials (*e.g.*, teeth) to fulfill the mechanical requirements. For example, Studart *et al.* developed a magnetic field-based method to alter the orientational and spatial distribution of reinforcing particles to give better structural design in artificial abrasion-resistant materials.[50] The ultrahigh magnetic response (UHMR) of nonmagnetic reinforcing particles (*e.g.*, alumina platelets) can be obtained by adsorbed sub-monolayer of superparamagnetic (*e.g.*, iron oxide) nanoparticles. By applying linear, uniform magnetic fields to fluid suspensions (polyurethane-based composites), homogeneously reinforced polymers can be fabricated (Fig. 11A). Then, multilayer composites can be further obtained by integrating laminar polymer with reinforced elements in different orientations (Fig. 11B). Compared to perpendicular reinforced and non-reinforced samples, samples with reinforcing particles oriented parallel to the applied load showed increased hardness (Fig. 11C), which is benefit for promoting the abrasion resistance of materials (Fig. 11D). More interestingly, the flexural modulus and surface hardness of heterogeneous epoxy-based bilayer composites can be simultaneously enhanced if the local orientation of reinforcing particles within each layer is tuned to mimic the overall architecture found in the tooth (highlighted by red dashed line in Fig. 11E). Therefore, it provides a promising strategy to the abrasion resistance of materials by preparing multilayer materials inspired by tooth.

5.4 Diatom inspired abrasion-resistant materials

In addition to usual multilayered structures, there are also non-layered structures (*e.g.*, porous structures) in natural materials with excellent abrasion-resistant property. Inspired by diatoms, Greer and his coworkers fabricated periodically arranged hollow titanium nitride (TiN) nanolattices with the dimensions of individual components varying from nanometers to hundreds of micrometers,[43] similar to those of cell walls in diatoms. They employed multi-step nanofabrication process to create 3D hollow ceramic scaffolds. Firstly, design of a 3D structure by using a computer design. Then, 3D solid polymer skeletons are generated by directly laser writing of this pattern into a photopolymer using two-photon lithography (Fig. 12A). Later, TiN are conformally deposited by means of atomic layer deposition (Fig. 12C). Finally, hollow ceramic nanolattices can be prepared by etching out of the

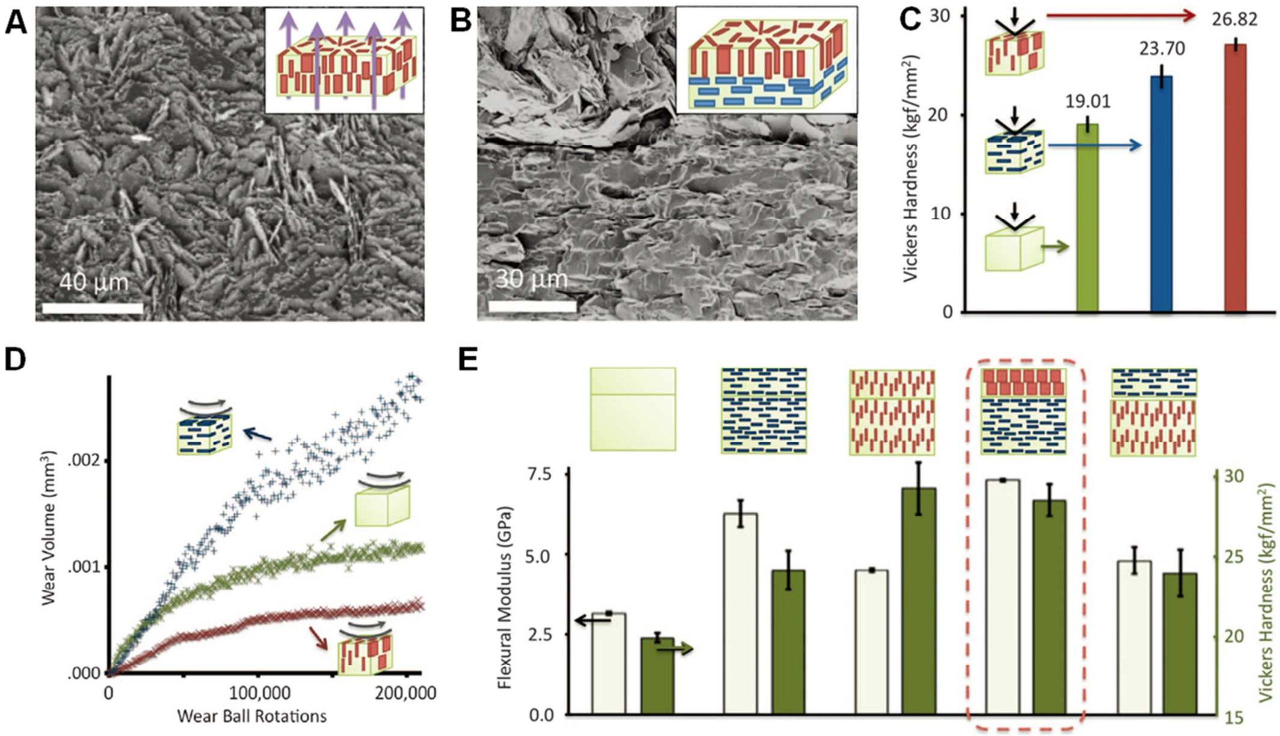

Fig. 11 (A) Out-of plane alignment of UHMR alumina platelets in polyurethane-based composites made with an out-of-plane magnetic field. (B) The cross section of laminated layers of in- and out-of-plane reinforced composites. (C) Increased hardness of resins reinforced with Al_2O_3 platelets parallel to the applied load versus perpendicular and non-reinforced samples. (D) Increased wear resistance for resins reinforced with out-of-plane aligned Al_2O_3 reinforcement. (E) The flexural modulus and surface hardness of heterogeneous epoxy-based bilayer composites exhibit different reinforcement architectures. Both properties can be simultaneously enhanced if the local orientation of reinforcing particles within each layer is tuned to mimic the overall architecture found in the tooth (highlighted by red dashed line). Adapted from ref. 50 Copyright 2012, American Association for the Advancement of Science.

polymer core (Fig. 12B). For monotonic loading, the load displacement curve in Fig. 12D shows that the samples maintain the elastic deformation, until fail at a maximum load of ca. 150 µN. These results show that hierarchical design principles inspired by diatoms are likely to build damage-tolerant lightweight engineering materials.

6. Conclusion and Outlook

In this review, we have summarized the recent progress of natural abrasion-resistant materials, showing that their unique abrasion-resistant property strongly depends on the correlation between chemical components and structural features. Current researches mainly focused on the characterization of chemical components and micro/nano-structures of natural abrasion-resistant materials, attempting to uncover the relationship between the abrasion-resistant property and natural design principles (Fig. 13). It is generally accepted that the cooperative effect of chemical components and micro/nano-structures is possibly responsible for their unique abrasion-resistant property. For example, in nacreous layer of gastropod,[8] the ordered aragonite platelets reinforce natural materials and enhance their mechanical strength. Meanwhile, organic components chitin and collagen act as buffer layer and/or adhesive layer to reduce external impaction and inhibit fracture during the abrasion process. To some extent, these progresses have just started to activate the development of this new field and help us to solve practical problems. However, it is still unclear that how these natural materials combine chemical components with micro/nano-structures to realize their unique abrasion-resistant property. To disclose these natural design principles and reproduce natural achievements, three crucial challenges should be considered in advance: i) to explore adequate natural abrasion-resistant examples for revealing their general design principles; ii) to devise effective methods for thoroughly characterizing the sophisticated natural materials; and iii) to create advanced synthetic and assembling technologies for the fabrication of bio-inspired materials which is more close to natural materials.

Although a few natural abrasion-resistant examples have been investigated, more efforts should be made for further understanding the design principles of natural materials with abrasion-resistant property. Firstly, it needs to explore and discover novel abrasion-resistant materials from nature so that we can build sufficient models to reveal their general design principles. Moreover, due to the exceeding complexity of natural materials, it is still difficult to precisely uncover the exact roles of their chemical components and micro/nano-structures and their inherent

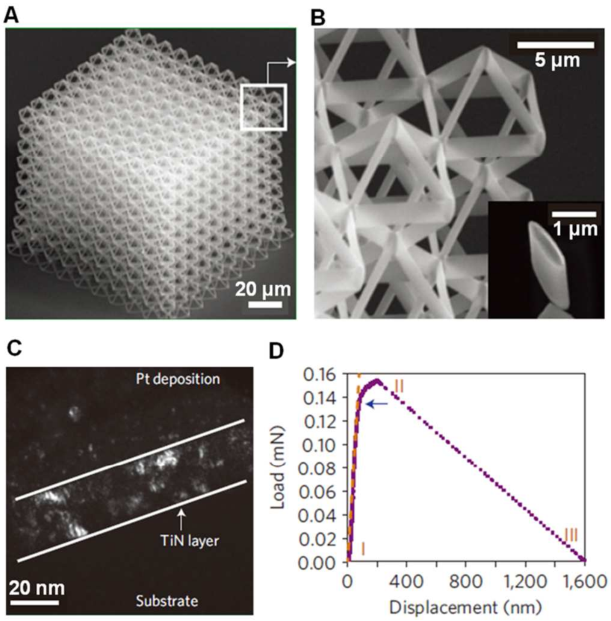

Fig. 12 (A) SEM and (B) enlarged SEM images of an engineered hollow nanolattice synthesized with TiN. (C) TEM images show the TiN thin film was deposited in the same batch with the nanolattice samples. (D) Load versus displacement data from a monotonic-loading experiment. Adapted from ref. 43 Copyright 2013, Macmillan Publishers Limited.

cooperative mechanism by using traditional characterization techniques. Therefore, it will be undoubtedly important to devise effective techniques and methods for thoroughly characterizing the sophisticated natural materials. One possible solution is to combine multiple advanced 3D characterization technologies, such as Nano CT and Tomography, with current techniques (*e.g.*, EDS mapping) for validating the roles of each parts. Another noteworthy aspect is to observe the dynamic changes of these chemical components and micro/nano-structures during the abrasion process, which are crucial for the understanding of their cooperative effect. Integrating computational approaches (*e.g.*, valence force field molecular dynamics[39]) with dynamic characterization methods (*e.g.*, *in-situ* small-angle X-ray scattering[36]) will offer an alternative way to further understand their design principles.

In addition, recent synthetic and assembling technologies are far from reproducing these sophisticated materials, due to the lack of systematic methodology for dealing with the structural complexity of natural materials whose dimensions span from nanoscale to macroscale. In recent years, the exploration of new biological abrasion-resistant materials and the rapid development of nanochemistry and microfabrication technologies provide us opportunities to explore and develop artificial abrasion-resistant materials beyond nature. By employing natural design principle, a promising strategy is proposed as shown in Fig. 13. For example, by employing artificial counterparts of chemical components (*e.g.*, polyurethane, dopa and chitosan) and structural units (*e.g.*, TiO_2 platelets, carbon nanotubes and Al_2O_3 rods), bio-inspired abrasion-

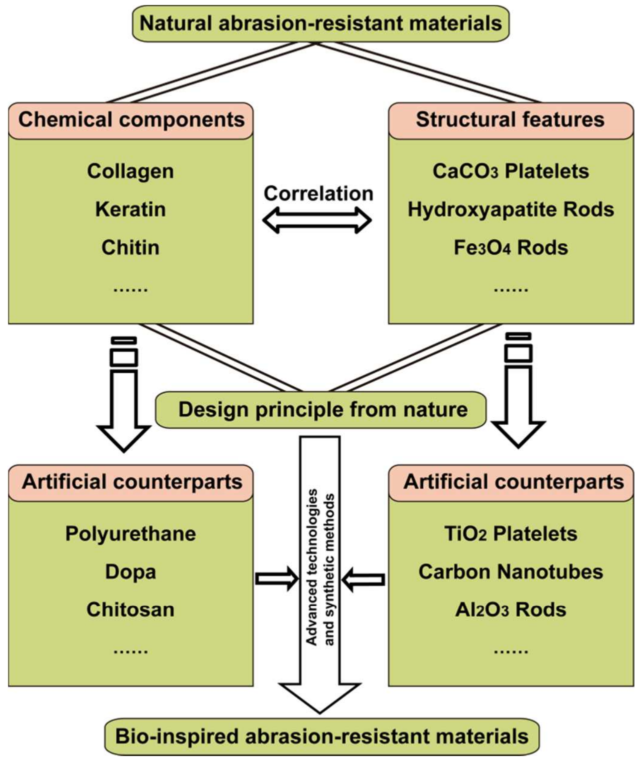

Fig. 13 Schematic proposed route of bio-inspired abrasion-resistant materials (learning from nature). Natural abrasion-resistant materials are fabricated from the cooperative effect of chemical components (*e.g.*, collagen) and structural features (*e.g.*, $CaCO_3$ platelets). Through multiple characterization methods, the natural design principles can be revealed. The artificial counterparts of chemical components and structural features are integrated with natural design principles, bio-inspired abrasion-resistant materials can be fabricated with suitable synthetic and assembling technologies.

resistant materials with tunable properties can be successfully fabricated. Another important example is the latest developed 3D-printing techniques, which offer much opportunity to create bio-inspired abrasion-resistant material according to the natural design principle. The progress brings out new opportunity to the development of new artificial materials with abrasion-resistant property.

Nature is the endless source of inspirations for fabricating novel functional materials. The exploration of natural systems will provide new research models, design principle, and building blocks for us to create novel artificial advanced materials. With the help of new characterization technologies and manufacturing methods, we are able to revisit the old natural systems of abrasion-resistant materials and activate the field of bio-inspired abrasion-resistant materials. We believe that bio-inspired abrasion-resistant materials will have a promising future under the guidance of learning from nature and assistance by advanced engineering technologies.

Acknowledgements

This research is supported by the National Research Fund for Fundamental Key Projects (2012CB933800), National Natural Science Foundation (21175140, 21425314, 21434009 and 21421061), the Key Research Program of the Chinese Academy of Sciences (KJZD-EW-M01), the National High Technology Research and Development Program of China (863 Program) (2013AA032203), MOST (2013YQ190467). We acknowledge Hongliang Liu and Junbing Fan for discussing the organization of the article.

References

1. B. Bhushan, *Principles and applications of tribology*, 2nd edn., JohnWiley & Sons, Ltd, 2013.
2. W. D. Sproul, *Science*, 1996, **273**, 889-892.
3. U. G. K. Wegst, H. Bai, E. Saiz, A. P. Tomsia and R. O. Ritchie, *Nat. Mater.*, 2015, **14**, 23-36.
4. Y. Seki, M. S. Schneider and M. A. Meyers, *Acta Mater.*, 2005, **53**, 5281-5296.
5. J. C. Weaver, Q. Wang, A. Miserez, A. Tantuccio, R. Stromberg, K. N. Bozhilov, P. Maxwell, R. Nay, S. T. Heier, E. DiMasi and D. Kisailus, *Mater. Today*, 2010, **13**, 42-52.
6. J. C. Weaver, G. W. Milliron, A. Miserez, K. Evans-Lutterodt, S. Herrera, I. Gallana, W. J. Mershon, B. Swanson, P. Zavattieri, E. DiMasi and D. Kisailus, *Science*, 2012, **336**, 1275-1280.
7. C. Tamerler and M. Sarikaya, *MRS Bulletin*, 2008, **33**, 504-512.
8. F. Heinemann, M. Launspach, K. Gries and M. Fritz, *Biophys. Chem.*, 2011, **153**, 126-153.
9. B. J. F. Bruet, J. H. Song, M. C. Boyce and C. Ortiz, *Nat. Mater.*, 2008, **7**, 748-756.
10. J. Aizenberg, J. C. Weaver, M. S. Thanawala, V. C. Sundar, D. E. Morse and P. Fratzl, *Science*, 2005, **309**, 275-278.
11. G. W. Greene, X. Banquy, D. W. Lee, D. D. Lowrey, J. Yu and J. N. Israelachvili, *Proc. Natl. Acad. Sci. USA*, 2011, **108**, 5255-5259.
12. N. D. Spencer, *Aqueous Lubrication: Natural and Biomimetic Approaches*, World Scientific Publishing Co. Pte. Ltd., Singapore, 2014.
13. J. F. Archard, *J. Appl. Phys.*, 1953, **24**, 981-988.
14. H. C. Lichtenegger, T. Schoberl, J. T. Ruokolainen, J. O. Cross, S. M. Heald, H. Birkedal, J. H. Waite and G. D. Stucky, *Proc. Natl. Acad. Sci. USA*, 2003, **100**, 9144-9149.
15. F. W. Zok and A. Miserez, *Acta Mater.*, 2007, **55**, 6365-6371.
16. S. Amini and A. Miserez, *Acta Biomater.*, 2013, **9**, 7895-7907.
17. A. Miserez, J. C. Weaver, P. J. Thurner, J. Aizenberg, Y. Dauphin, P. Fratzl, D. E. Morse and F. W. Zok, *Adv. Funct. Mater.*, 2008, **18**, 1241-1248.
18. W. C. Oliver and G. M. Pharr, *J. Mater. Res.*, 1992, **7**, 1564-1583.
19. F. Bouville, E. Maire, S. Meille, B. Van de Moortele, A. J. Stevenson and S. Deville, *Nat. Mater.*, 2014, **13**, 508-514.
20. Y. Politi, M. Priewasser, E. Pippel, P. Zaslansky, J. Hartmann, S. Siegel, C. Li, F. G. Barth and P. Fratzl, *Adv. Funct. Mater.*, 2012, **22**, 2519-2528.
21. S. Bentov, P. Zaslansky, A. Al-Sawalmih, A. Masic, P. Fratzl, A. Sagi, A. Berman and B. Aichmayer, *Nat. Commun.*, 2012, **3**, 839.
22. M. J. Harrington, A. Masic, N. Holten-Andersen, J. H. Waite and P. Fratzl, *Science*, 2010, **328**, 216-220.
23. Y. Ma, S. R. Cohen, L. Addadi and S. Weiner, *Adv. Mater.*, 2008, **20**, 1555-1559.
24. M. G. Pontin, D. N. Moses, J. H. Waite and F. W. Zok, *Proc. Natl. Acad. Sci. USA*, 2007, **104**, 13559-13564.
25. E. Degtyar, M. J. Harrington, Y. Politi and P. Fratzl, *Angew. Chem. Int. Ed.*, 2014, **53**, 12026-12044.
26. J. Y. Rho, L. Kuhn-Spearing and P. Zioupos, *Med. Eng. Phys.*, 1998, **20**, 92-102.
27. I. H. Chen, W. Yang and M. A. Meyers, *Mater. Sci. Eng. C*, 2014, **35**, 441-448.
28. L. C. Palmer, C. J. Newcomb, S. R. Kaltz, E. D. Spoerke and S. I. Stupp, *Chem. Rev.*, 2008, **108**, 4754-4783.
29. I. H. Chen, J. H. Kiang, V. Correa, M. I. Lopez, P.-Y. Chen, J. McKittrick and M. A. Meyers, *J. Mech. Behav. Biomed. Mater.*, 2011, **4**, 713-722.
30. P. Y. Chen, J. McKittrick and M. A. Meyers, *Prog. Mater. Sci.*, 2012, **57**, 1492-1704.
31. L. Li and C. Ortiz, *Nat. Mater.*, 2014, **13**, 501-507.
32. A. Al-Sawalmih, C. Li, S. Siegel, H. Fabritius, S. Yi, D. Raabe, P. Fratzl and O. Paris, *Adv. Funct. Mater.*, 2008, **18**, 3307-3314.
33. C. E. Hamm, R. Merkel, O. Springer, P. Jurkojc, C. Maier, K. Prechtel and V. Smetacek, *Nature*, 2003, **421**, 841-843.
34. H. M. Yao, M. Dao, T. Imholt, J. M. Huang, K. Wheeler, A. Bonilla, S. Suresh and C. Ortiz, *Proc. Natl. Acad. Sci. USA*, 2010, **107**, 987-992.
35. B. Achrai, B. Bar-On and H. D. Wagner, *Bioinspir. Biomim.*, 2015, **10**, 016009.
36. E. A. Zimmermann, B. Gludovatz, E. Schaible, N. K. N. Dave, W. Yang, M. A. Meyers and R. O. Ritchie, *Nat. Commun.*, 2013, **4**, 2634.
37. S. Krauss, E. Monsonego-Ornan, E. Zelzer, P. Fratzl and R. Shahar, *Adv. Mater.*, 2009, **21**, 407-412.
38. H. O. Fabritius, C. Sachs, P. R. Triguero and D. Raabe, *Adv. Mater.*, 2009, **21**, 391-400.
39. S. Nikolov, M. Petrov, L. Lymperakis, M. Friak, C. Sachs, H. O. Fabritius, D. Raabe and J. Neugebauer, *Adv. Mater.*, 2010, **22**, 519-526.
40. J. F. V. Vincent and U. G. K. Wegst, *Arthropod Struct. Dev.*, 2004, **33**, 187-199.
41. J. G. Fernandez and D. E. Ingber, *Adv. Mater.*, 2012, **24**, 480-484.
42. J. Sun and B. Bhushan, *RSC Advances*, 2012, **2**, 7617-7632.
43. D. Jang, L. R. Meza, F. Greer and J. R. Greer, *Nat. Mater.*, 2013, **12**, 893-898.
44. A. Miserez, J. C. Weaver, P. B. Pedersen, T. Schneeberk, R. T. Hanlon, D. Kisailus and H. Birkedal, *Adv. Mater.*, 2009, **21**, 401-406.
45. W. Yang, I. H. Chen, B. Gludovatz, E. A. Zimmermann, R. O. Ritchie and M. A. Meyers, *Adv. Mater.*, 2013, **25**, 31-48.
46. P. Y. Chen, A. Y.-M. Lin, J. McKittrick and M. A. Meyers, *Acta Biomater.*, 2008, **4**, 587-596.
47. Y. S. Lin, C. T. Wei, E. A. Olevsky and M. A. Meyers, *J. Mech. Behav. Biomed.*, 2011, **4**, 1145-1156.
48. V. Imbeni, J. J. Kruzic, G. W. Marshall, S. J. Marshall and R. O. Ritchie, *Nat. Mater.*, 2005, **4**, 229-232.
49. E. Munch, M. E. Launey, D. H. Alsem, E. Saiz, A. P. Tomsia and R. O. Ritchie, *Science*, 2008, **322**, 1516-1520.
50. R. M. Erb, R. Libanori, N. Rothfuchs and A. R. Studart, *Science*, 2012, **335**, 199-204.

Table of contents entry

The recent investigations of natural abrasion-resistant materials for exploring their general design principle and fabricating bio-inspired abrasion-resistant materials are reviewed.

.